JOC Article

Conformational Flexibility of Corey Lactone Derivatives Indicated by Absorption and Vibrational Circular Dichroism Spectra

Zuzana Tománková,[†] Vladimír Setnička,[†] Marie Urbanová,[‡] Pavel Matějka,[†] Vladimír Král,[†] Karel Volka,[†] and Petr Bouř*,[†,§]

Department of Analytical Chemistry and Department of Physics and Measurement, Institute of Chemical Technology, Technická 5, 16628 Praha 6, Czech Republic, and Institute of Organic Chemistry and Biochemistry, Academy of Sciences of the Czech Republic, Flemingovo nám. 2, 16610 Praha 6, Czech Republic

bour@uochb.cas.cz

Received July 28, 2003

Infrared absorption and vibrational circular dichroism (VCD) spectra of four Corey lactone derivatives (diol, benzoate, *p*-phenylbenzoate, and bisbenzoate) were measured and analyzed on the basis of ab initio computations. The analysis interpreted most of the spectral features as well as the differences among individual compounds. Despite the common rigid lactone residue, conformational behaviors and spectral features of the derivatives were found to be different, because of hydrogen bonding and solvent effects. Recognition of common molecular parts in the spectra of different molecules increases the potential of using VCD for monitoring the purity of intermediates in chiral syntheses. For the derivatives, a conserved spectral component corresponding to the lactone skeleton could be identified on the basis of theoretical analysis but was relatively weak in intensity.

Introduction

The Corey lactone serves as a starting compound for the synthesis of prostaglandin derivatives and is widely used in the pharmaceutical industry.[1−3] Prostaglandins are natural lipid mediators of physiological processes including modulation of inflammation, ovulation, arterial blood pressure, and immunity.[4,54−5] Purification of its synthetic intermediates is based on enzymatic hydrolysis[6] or crystallization of diastereoisomers from solution.[7] Vibrational circular dichroism (VCD),[8] which is sensitive to enantiomeric purity and conformation, is thus a potential tool to conveniently monitor these steps in the solution process.

Fundamental, instrumental, and theoretical aspects of VCD have been established. Particularly, the magnetic field perturbation theory of Stephens[9,10] implemented at the density functional theory (DFT) level and combined with magnetic field dependent atomic orbitals[11] has been implemented in the Gaussian 98[12] and other program packages, which made simulations and interpretation of the spectra easier. For small rigid molecules within the harmonic approximation, such VCD simulations are normally very accurate in the mid-IR region.[13−15] However, for systems that strongly interact with the solvent or exhibit conformational flexibility, the analysis of VCD spectra is far from being straightforward. This is caused partially by inadequacies in the theoretical models for such systems. In fact, there are only a few works dealing with the analysis of the spectra of flexible molecules. This often requires multidimensional analysis of the conformational space[16,17] and combination of VCD with data

[†] Department of Analytical Chemistry, Institute of Chemical Technology.

[‡] Department of Physics and Measurement, Institute of Chemical Technology.

[§] Institute of Organic Chemistry and Biochemistry, Academy of Sciences of the Czech Republic.

(1) Harris, S. G.; Padilla, J.; Koumas, L.; Ray, D.; Phipps, R. P. *Trends Immunol.* **2002**, *23*, 144.

(2) Irie, T.; Tsujii, M. *Horumon to Rinsho* **2002**, *50*, 253.

(3) Bertolini, A.; Ottani, A.; Sandrini, M. *Pharm. Res.* **2001**, *44*, 437.

(4) Breyer, R. M.; Kennedy, C. R. J.; Zhang, Y.; Breyer, M. D. *Ann. N. Y. Acad. Sci.* **2000**, *905*, 221.

(5) Peskar, B. M. *J. Physiol. Pharmacol.* **2001**, *52*, 555.

(6) Theil, F.; Schick, H.; Nedkov, P.; Boehme, M.; Haefner, B.; Schwarz, S. *J. Prakt. Chem./Chem.-Ztg.* **1988**, *330*, 893.

(7) Žák, B.; Veselý, I.; Neumitka, K.; Paleček, J. *Collect. Czech. Chem. Commun.* **1991**, *56*, 1690.

(8) Barron, L. D. *Molecular Light Scattering and Optical Activity*; Cambridge University Press: Cambridge, England, 1982.

(9) Stephens, P. J. *J. Phys. Chem.* **1985**, *89*, 748.

(10) Stephens, P. J. *J. Phys. Chem.* **1987**, *91*, 1712.

(11) Stephens, P. J.; Ashvar, C. S.; Devlin, F. J.; Cheeseman, J. R.; Frisch, M. J. *Mol. Phys.* **1996**, *89*, 579.

(12) Frisch, M. J.; Trucks, G. W.; Schlegel, H. B.; Scuseria, G. E.; Robb, M. A.; Cheeseman, J. R.; Zakrzewski, V. G.; Montgomery, J. A.; Stratmann, R. E.; Burant, J. C.; Dapprich, S.; Millam, J. M.; Daniels, A. D.; Kudin, K. N.; Strain, M. C.; Farkas, O.; Tomasi, J.; Barone, V.; Cossi, M.; Cammi, R.; Mennucci, B.; Pomelli, C.; Adamo, C.; Clifford, S.; Ochterski, J.; Petersson, G. A.; Ayala, P. Y.; Cui, Q.; Morokuma, K.; Malick, D. K.; Rabuck, A. D.; Raghavachari, K.; Foresman, J. B.; Cioslowski, J.; Ortiz, J. V.; Stefanov, B. B.; Liu, G.; Liashenko, A.; Piskorz, P.; Komaroni, I.; Gomperts, R.; Martin, R. L.; Fox, D. J.; Keith, T.; Al-Laham, M. A.; Peng, C. Y.; Nanayakkara, A.; Gonzales, C.; Challacombe, M.; Gill, P. M. W.; Johnson, B. G.; Chen, W.; Wong, M. W.; Andres, J. L.; Head-Gordon, M.; Replogle, E. S.; Pople, J. A. *Gaussian 98*, revision A.7; Gaussian, Inc.: Pittsburgh, PA, 1998.

(13) Stephens, P. J.; Devlin, F. J.; Chabalowski, C. F.; Frisch, M. J. *J. Phys. Chem.* **1994**, *98*, 11623.

(14) Bouř, P.; McCann, J.; Wieser, H. *J. Phys. Chem. A* **1997**, *101*, 9783.

(15) Bouř, P.; McCann, J.; Wieser, H. *J. Phys. Chem. A* **1998**, *102*, 102.

(16) Devlin, F. J.; Stephens, P. J.; Scafato, P.; Superchi, S.; Rosini, C. *J. Phys. Chem. A* **2002**, *106*, 10510.

(17) Wang, F.; Polavarapu, P. L.; Lebon, F.; Longhi, G.; Abbate, S.; Catellani, M. *J. Phys. Chem. A* **2002**, *106*, 12365.

10.1021/jo035099h CCC: $27.50
Published on Web 12/11/2003

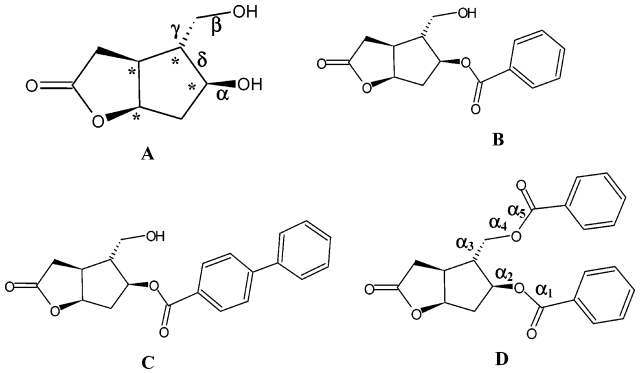

FIGURE 1. Corey lactone derivatives studied here: **A**, (+)-Corey lactone diol, asymmetric carbons marked by asterisk (∗); **B**, (+)-Corey lactone benzoate alcohol; **C**, (+)-Corey lactone *p*-phenylbenzoate alcohol; **D**, (−)-Corey lactone bisbenzoate. Flexible bonds (torsion angles as in Tables 2S and 3S in the Supporting Information) are labeled for **A** and **D**.

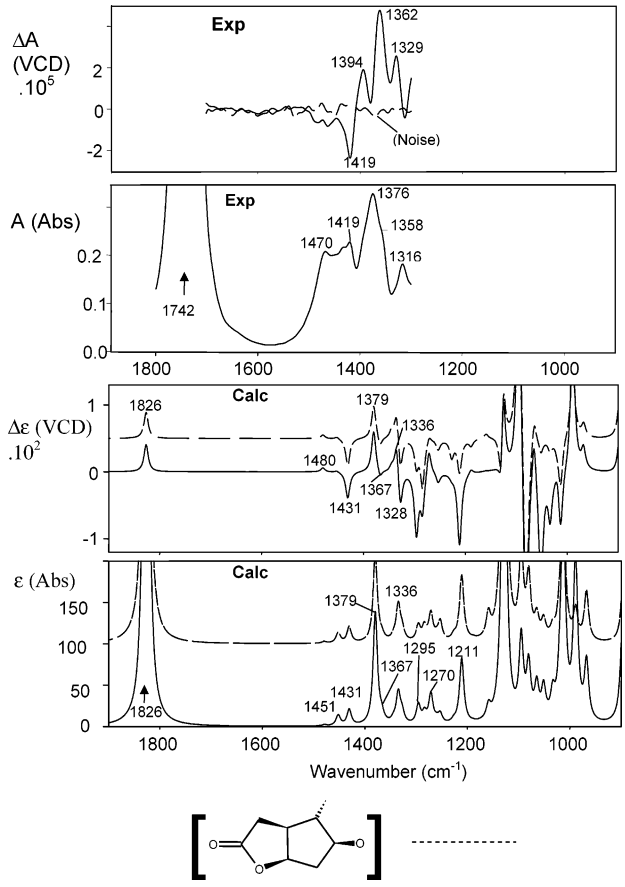

FIGURE 2. Experimental (in D_2O) and calculated (BPW91/6-31G**) VCD and absorption spectra of the Corey lactone diol **A**. Contributions of the lactone core atoms (indicated in the brackets [ ] in the lower part) to the calculated spectra are drawn by the vertically offset dashed lines.

from other spectroscopic techniques.[18] Similarly, the availability of a series of compounds, as in the case of the Corey lactone derivatives, enhances the analysis and provides a more complete picture about a general applicability of VCD for structural studies of chiral organic molecules.

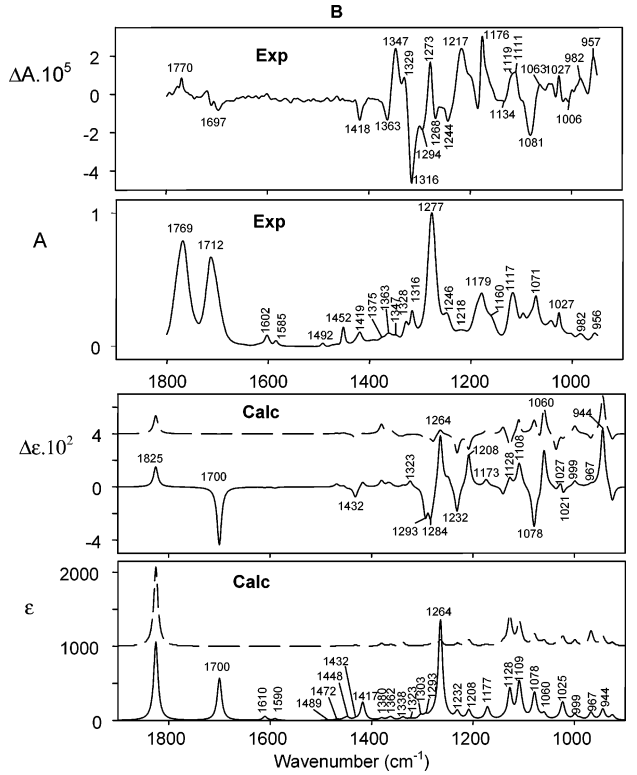

FIGURE 3. Experimental (top, in $CDCl_3$) and calculated (bottom, BPW91/6-31G**) VCD and absorption spectra of the Corey lactone benzoate **B**. Contributions of the lactone core atoms to the spectra are drawn by the dashed lines as in Figure 1.

The series also makes it possible to test the transferability concept in infrared spectroscopy. Characteristic bands often indicate the presence of particular functional groups in molecules. Such "fingerprinting", however, often breaks down in VCD,[19] because of coupling between the chromophores, which can lead to a chiral interaction not represented in the transfer. In the case of the lactones, the bicyclic system is relatively rigid, and its marker bands, although weak, can be identified in the spectra of various derivatives as shown in this paper.

Results and Discussion

Experimental Spectra. Experimental IR and VCD spectra of the compounds (structures in Figure 1) are presented in the upper parts of Figures 2−5. For **A** (Figure 2), only a narrow range of frequencies was accessible as a result of the D_2O solvent, because the diol was not sufficiently soluble in the more transparent $CDCl_3$. Estimation of the noise in the experimental VCD spectrum is given as the dashed line. Noise levels for the other compounds (data not shown) were similar. As can be seen in Figures 3−5, experimental spectra of the derivatives **B**−**D** possess many common features in both IR (the three strongest bands around 1770, 1710, and 1275 cm^{-1}) and VCD (the + − − + pattern at ∼1347, 1314, 1242, and 1178 cm^{-1}, respectively) spectra. However, the relation of their spectra to those of the parent compound **A** is not obvious.

(18) Bouř, P.; Navratilová, H.; Setnička, V.; Urbanová, M.; Volka, K. *J. Org. Chem.* **2002**, *67*, 161.

(19) Rauk, A.; McCann, J.; Wieser, H.; Bouř, P.; El'natanov, Y. I.; Kostyanovsky, R. G. *Can. J. Chem.* **1998**, *76*, 717.

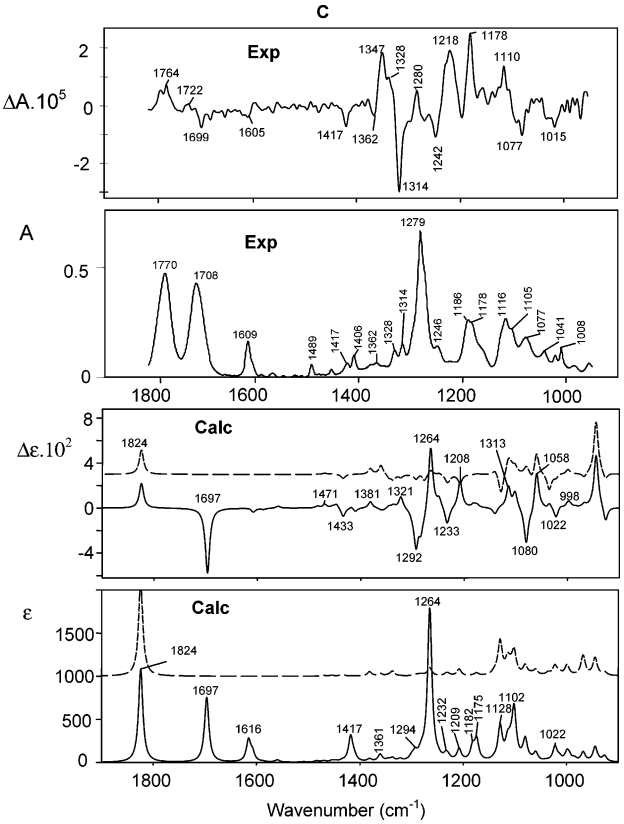

FIGURE 4. Experimental (in $CDCl_3$) and calculated (BPW91/6-31G**) VCD and absorption spectra of the Corey lactone *p*-phenylbenzoate **C**. Contributions of the lactone core atoms are drawn by the dashed lines as in Figure 1.

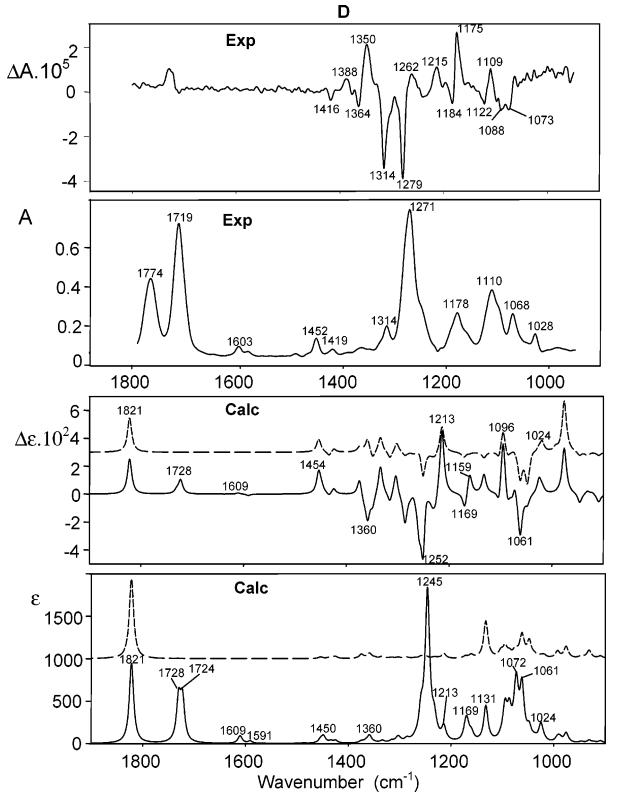

FIGURE 5. Experimental ($CDCl_3$) and calculated (BPW91/6-31G**) VCD and absorption spectra of the Corey lactone bisbenzoate **D**. Contributions of the lactone core atoms are drawn by the dashed lines as in Figure 1.

Theoretical Spectra. In the lower parts of Figures 2−5, VCD and absorption spectra for the four derivatives as calculated at the BPW91/6-31G** level are presented for lowest-energy conformations only. Supposedly, these conformations are the most populated and thus provide a first-order approximation, on the basis of which most of the observed IR and some VCD spectral features can be explained. For VCD, bigger differences between the calculation and experiment are anticipated than those for the absorption spectra, mainly for compounds **A** and **D**, because of the higher sensitivity of the VCD signal to conformational freedom.

To enhance the mode analysis, we also separated the theoretical contributions of the lactone bicyclic ring atoms (see the bottom of Figure 2) to spectral intensities and drew them as dashed lines. The dashed-line spectra were thus obtained by setting all of the atomic polar and axial tensors (determining the spectral intensities) to zero for atoms not contained in the rigid lactone residue. Note that vibrational frequencies, unlike intensities, are unchanged during this procedure; particularly lactone and side-chain vibrational modes can still couple. As expected, the reduced spectrum obtained in this way is almost equal to the original spectrum of derivative **A**, because in that case only three atoms (the HO group and H) were deleted. On the contrary, for **B**−**D**, the VCD of the lactone part of the molecule is for most bands much smaller than that coming from the aromatic residues. This obviously explains the difference in the overall character of the spectra for **A**, if compared to **B**−**D**. Another interesting feature is that both the lactone and aromatic residues contribute to most of the mid-IR bands. In other words, the spectrum is not just a sum of the spectra from the two chromophores, because of the coupling of their vibrational modes. Finally, we can also observe that the relative contribution of the lactone residue is bigger in the VCD spectra than in absorption. This can be also explained because the aromatic residues are not inherently chiral, and their eventual chiral behavior is entirely determined by the lactone with the four asymmetric carbons. For **C**, the twisted biphenyl group is generally chiral but, according to the calculations, does not contribute significantly to the VCD intensities in the analyzed region of the frequencies. Because of the low energies associated with its rotation, the signal is further weakened by a temperature averaging. Indeed, the VCD sign pattern for **B** and **C** is virtually identical both for the experiment and for the calculated spectra, proving that the additional phenyl residue is virtually invisible in VCD.

Mode Assignment. Detailed assignment of the most intense vibrational transitions based on the comparisons in Figures 2−5 is listed in Table 1. Quite a good agreement for the theoretical and absorption profile of derivative **A** can be observed in Figure 2, and most of the transitions can be assigned. The carbonyl frequency was rather overestimated, but this can be clearly attributed to the formation of hydrogen bonds in D_2O. The frequencies of other bands (1470−1316 cm^{-1}) were calculated with much smaller error (~1%), and their relative intensities were predicted correctly, with the intensity of the calculated peak at 1379 cm^{-1} being too big. The assignment of most vibrational modes (Table 1) can be

TABLE 1. Comparison of Experimental and Calculated Frequencies (in cm^{-1}) for the Three Corey Lactone Derivatives and the Mode Assignment

compound	IR	VCD	BPW91/6-31G**	
A	1742		1826	ν(C═O)
	1470		1451	CH_2 scissoring
	1419	1419 (−)	1434, 1431	CH_2 scissoring
	1376	1394 (+), 1362 (+)	1379	CH_2 and CH wagging
	1358		1367	CH_2 and CH wagging
	1316	1329 (+)	1336	ν(C−O), ring def. and CH wag
			1328	ring def., CH bend
B	1770	1770 (+)	1825	ν(C═O), lactone
	1712	1697 (−)	1700	ν(C═O), ester
	1602, 1585	(−)	1610, 1590	ν(C═C), phenyl
	1492−1450	(+)	1489−1417	ν(C═C), CH bend, phenyl
	1419	1418 (−)	1432	CH_2 scissoring
			1417	$-CH_2OH$ H bending
	1375−1347	1347 (+)	1380−1323	CH bending modes, lactone
	1303		1328	CH bend, phenyl
	1316	1316 (−)	1293	CH bend, lactone
		1294 (−)	1294, 1284	CH bend, ν(CO−C), lactone
	1277	1273 (+)	1264	ν(CO−C), ester
	1246	1244 (−)	1232	$-CH_2OH$ bending
	1218	1217 (+)	1208	$-CH_2OH$ bending
	1179, 1160	1176 (+)	1172, 1161	phenyl def., CH bend
	1117	1119 (+)	1128	ν(CO−O), lactone
		1111 (+)	1109	ν(CO−O), ester
	1071	1081 (−)	1080	lactone, deloc.
			1078	phenyl C═C def.
	1027	1027 (+)	1026 (+), 1025 (−)	phenyl breathing, lactone ν(C−C)
	999		999	ν(C−O), ν(C−C), lactone
	982	928 (+)	967	ν(C−O) ester, lactone def.
	956	957 (+)	944	lactone deloc.
C	1770		1824	ν(C═O) (lactone)
	1708	1722 (+), 1699 (−)	1697	ν(C═O) (ArC═O)
	1609	1605 (−)	1616	ν(C═C) (Ar)
	1489		1471, 1449, 1433	CH_2 scissoring
	1417, 1406	1417 (−)	1417	CH_2 scissoring
	1362	1362 (−)	1381, 1361	CH_2 sciss. + CH wag.
	1328	1347 (+), 1328 (+)	1321	CH bend, both aliph. + arom.
	1314	1314 (−)	1292, 1294	ν(C−O), CH bend
	1279	1280 (+)	1264	ν(C−O) (Ar)
	1246	1242 (−)	1232	CH_2 wag + ring def.
		1218 (+)	1208	CH_2 wag + ring def.
	1186, 1178	1178 (+)	1182, 1175	CH bend Ar, lactone ring def.
	1116, 1105	1110 (+)	1113, 1101	ν(C−O) (Ar), lactone ring def.
	1077	1077 (−)	1080, 1058	ν(C−C), lactone ring def.
	1041	1030 (−)	1022	ν(C−C), lactone ring def.
	1008		998	ν(C−C) lactone ring def.
D	1774		1821	ν(C═O) (Corey)
	1719		1728, 1724	ν(C═O) (COO)
	1603, 1585	1605 (−)	1609, 1591	CH bend (Phe)
	1452		1450	CH_2 scissoring
	1419	1416 (−)	1420	CH_2 scissoring
	1360	1388 (+), 1364 (−)	1374, 1360	CH_2 wag and CH bend
		1350 (+)		
	1314	1314 (−)	1304	CH bend (Phe)
	1271	1279 (−)	1245	ν((Phe)C−C(═O))
	1248	1262 (+), 1215 (+)	1230, 1213	ν(C−C), lactone ring def.
	1178	1175 (+)	1161	CH_2 twist
		1122 (−)		
	1110	1109 (+)	1096	ν(C−O) (Ar)
	1099	1088 (−)	1061	ν(C−C), lactone ring def.
	1068	1073		
	1028		1024	lactone and Ar ring def.

confirmed on the basis of the VCD spectra. The experimental negative VCD band at 1419 cm^{-1} was calculated with the same sign at 1431 cm^{-1}. The observed splitting of bands at 1394 and 1362 cm^{-1} is not matched by the calculation, but the positive signal appears as a peak centered at 1379 cm^{-1}. The 1329 cm^{-1} positive signal most probably corresponds to the calculated positive peak at 1336 cm^{-1}.

For the derivatives **B**−**D**, the correspondence between calculated and experimental absorption spectra is obvious. Many spectral details were reproduced; for example, the frequency of the strongest aromatic C═C stretching signal in **C** (experimental at 1609 cm^{-1}, calculated at 1616 cm^{-1}) is higher than for **B** and **D** (experimental at ∼1602 cm^{-1}, calculated at ∼1609 cm^{-1}), and its intensity is much bigger. Similarly, the red shift of the most intense C−O stretching peak (from 1277−1279 cm^{-1} for **B**−**C** to 1271 cm^{-1} for **D**) is reproduced, although rather overestimated (1245−1264 cm^{-1}). The "fingerprint" absorption bands from **A** are relatively low in intensity for **B**−**D** but can be clearly seen in two regions: around 1360 cm^{-1}, where the contribution of the lactone CH_2 and CH wagging vibrations is located, and around 1100 cm^{-1}, where the lactone ring-deformation modes appear. The latter, however, is coupled with the C−O stretching of the substituent.

The lactone residue VCD bands are most important from the point of view of analytical chemistry. As can be

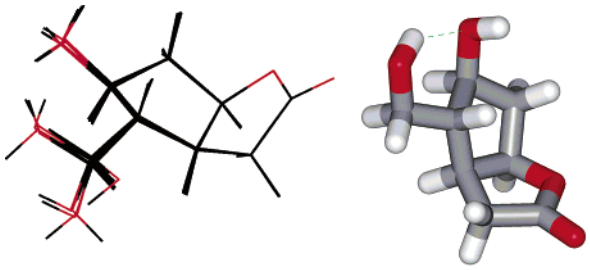

FIGURE 6. Left: the overlapped 10 lowest-energy conformers (1−10 in Table 2S in the Supporting Information). Right: the lowest-energy conformation (1) of diol **A**.

seen in Table 1 and Figures 2−5, the lactone carbonyl VCD signal (experimental at ~1700 cm^{-1}) is negative for **B** and **C** and positive for **D**, which was reproduced by the theory. Supposedly, the VCD sign of this band is determined by the dipolar coupling between the C═O lactone and ester chromophores in the molecule. The weak experimental negative signal around 1416−1419 cm^{-1} is common for all four derivatives and clearly stems from the CH_2 scissoring in the lactone skeleton. This is reproduced by the calculation at a slightly higher frequency (~1430 cm^{-1}). For **D**, this signal is perturbed by a positive peak calculated at 1454 cm^{-1} not observed in experiment. For all of the derivatives, there is another region of mostly positive VCD around 1328−1350 cm^{-1} in the experimental spectra, which is roughly reproduced by the calculation, especially if we suppose that the VCD from the flexible groups averages out. For **B**−**D**, the other common region of mostly negative VCD signal is located in the experimental spectra around 1073−1088 cm^{-1} and reproduced by the calculation at 1061−1081 cm^{-1}.

Conformational Flexibility. Despite the rough agreement, the VCD spectra for **A** and **D** clearly cannot be fully explained with only a one-conformer model. As follows from the systematic conformational analysis of the diol **A** (Table 2S in the Supporting Information and Figure 6), the lowest-energy conformation is dominant, which can be explained by an intramolecular hydrogen bond (Figure 4) and internal dipolar interactions among the OH groups and the carboxylic lactone residue. The lactone skeleton remains relatively rigid (with the exception of conformation 16), and the conformers differ by the orientation of the −OH and $-CH_2OH$ groups. However, substantial occurrence of other conformations (even with higher populations than those estimated in a vacuum in Table 2S in the Supporting Information) in the sample cannot be ruled out, because of the limited precision of the computations as well as because of the hydrogen bonding to the solvent. Especially at elevated temperatures, a semifree movement of the side groups can be expected. Because we cannot fully account for these effects, we may at least estimate the influence of the conformational flexibility on the spectra. This is done in Figure 7, where the VCD and absorption spectra of the 10 lowest-energy conformations are overlapped. Clearly, there are many regions both in the absorption and in the VCD where the spectra are almost unaffected by the conformational change, most notably the VCD negative signal at 1419 cm^{-1}. This is consistent with the above analysis, where this band was found to be conserved for all three compounds and assigned to a vibration of the rigid lactone skeleton. The dependence of the VCD signal of

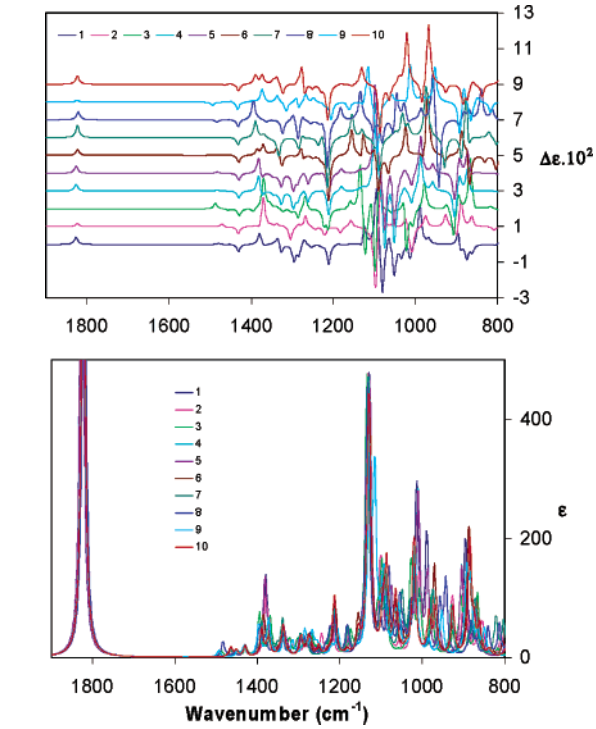

FIGURE 7. Simulated VCD (upper) and absorption (lower) spectra of the 10 lowest-energy conformations of diol **A**.

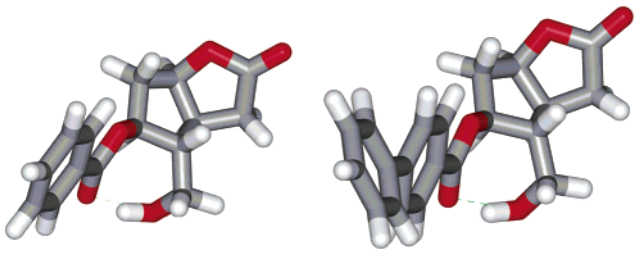

FIGURE 8. Optimized geometry (BPW91/6-31G**) of the derivatives **B** and **C**.

the C═O stretching (calculated at 1826 cm^{-1}) on the side-chain conformation is somewhat surprising, and normally one would not expect such a long-range influence on a relatively rigid carbonyl system. This is in accordance with the calculated relative energies of the conformers, predicting strong electrostatic interactions between the polar parts of the molecule. The VCD spectra are more sensitive to the conformation of the molecule than the absorption. However, if compared to similar previous studies,[13,14] the dependence is not so dramatic, and the basic VCD shape arises from the rigid skeleton. Absorption peaks above 1000 cm^{-1} do not significantly change their positions and intensities for various conformers; the absorption sensitivity on the conformation is unusually high for the signal around 950 cm^{-1}.

Not surprisingly, conformational flexibility of the derivatives **B** and **C** is quite similar. The geometries of their lowest-energy conformations are drawn in Figure 8. They are stabilized by intramolecular hydrogen bonds, similar to that for **A**. However, we did not find other conformers that could be present in higher amounts in the sample, except those stemming from the benzene ring rotation for **C**. This bisphenyl chromophore, however, does not contribute significantly to the spectra, because

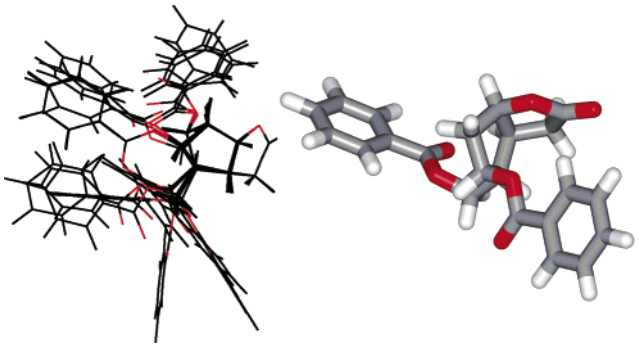

FIGURE 9. Nine (I−IX in Table 3S in the Supporting Information, left) lowest and the lowest (I, right) energy conformation of **D**.

of the small dipole strengths associated with its vibrations. Additionally, unlike **A**, we do not expect that the hydrogen bond would be disturbed by the solvent ($CDCl_3$), and thus we consider a one-conformation model sufficient for this compound. This is also consistent with the reasonable agreement between the calculated and experimental absorption and the VCD spectra (Figures 3 and 4). Because most of VCD signs are predicted correctly, relative differences between calculated and experimental VCD intensities can probably be attributed to the solvent effects and computational (BPW91/6-31G**) error rather than to the conformational freedom.

The last compound **D** cannot form intramolecular hydrogen bonds, and its flexible conformational behavior differs quite a bit from the previous cases. This can be seen in Table 3S in the Supporting Information, where the calculated relative energies of the nine lowest-energy conformers calculated at the molecular mechanics (MM), PM3, HF/3-21, and BPW91/6-31G** levels are given. Because of our computer limitations, higher energy (>2 kcal/mol in BPW91/6-31G**) conformers were not included; these, however, should not contribute significantly to the spectra because of their low population. Supposedly, the vacuum computations can also be extended to the sample dissolved in $CDCl_3$, where a formation of stable hydrogen bonds to the solvent is limited. As can be seen in Figure 9, the conformers differ only by the position of the benzoate residues, while the lactone bicyclic system remains relatively rigid, similarly for **A**−**C**. The lowest-energy "extended" conformation (I, right in Figure 9) has the polar as well as the phenyl residues separated, possibly because of the repellent dipolar interaction of the carboxylic groups.

The spectra of **D** (Figure 10) depend on the conformation somewhat differently than those of compound **A** (Figure 7): the absorption is less variable, while the VCD varies more. Because it is difficult to predict conformational ratios (energy differences smaller than 1 kcal/mol given in Table 3S in the Supporting Information almost certainly lie within the error of the BPW91/6-31G** method), as a first approximation to the experiment, we constructed the arithmetic average spectra from these nine conformations, shown on the right-hand side of Figure 8. A Boltzmann weighting (not shown) provided a qualitatively similar resultant spectrum. Note that the computation of VCD is quite time-consuming for this compound, and the number of the conformers had to be limited. As follows from the comparison with the lowest-conformation spectrum and with the experiment (Figure 5), the averaging brings a minor improvement for the absorption, consisting mainly of a more realistic intensity ratio for the C=O stretching bands and the profile of the broad signal around 1100 cm^{-1}. For VCD, however, the improvement is more substantial: the two experimental minima at 1416 and 1364 cm^{-1} as well as the maximum at 1350 cm^{-1} (calculated now at 1336 cm^{-1}) also appear in the theoretical spectrum, as do the strong negative

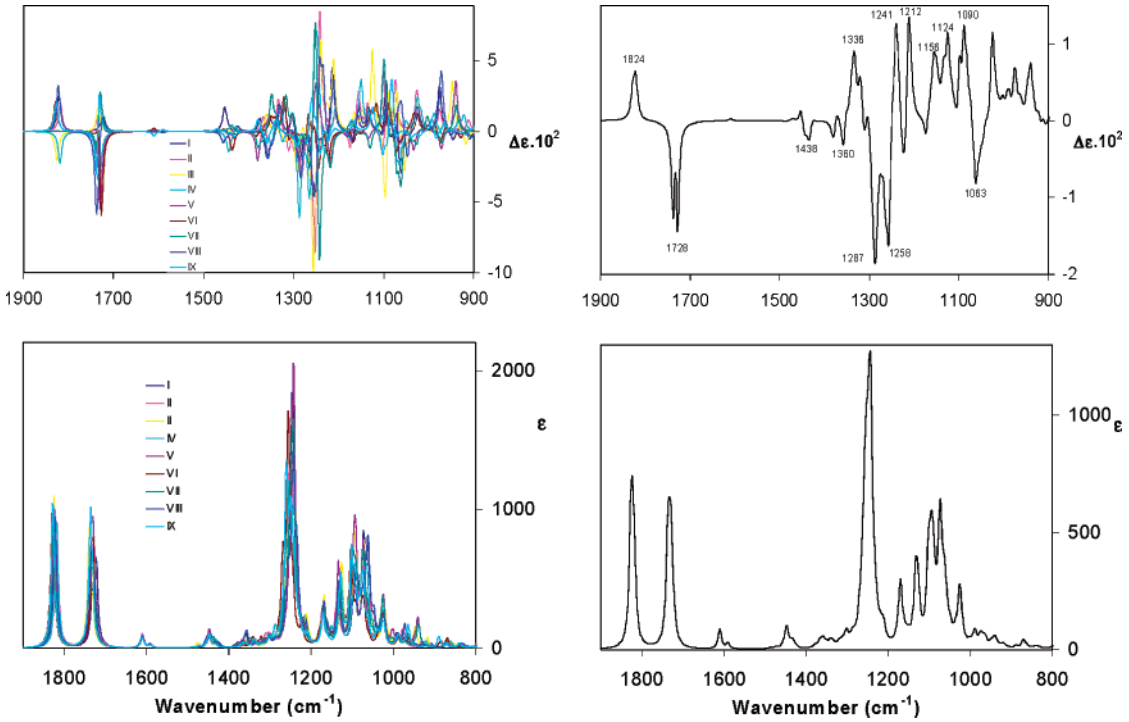

FIGURE 10. Bisbenzoate **D** calculated VCD (top) and absorption (bottom) spectra of nine conformers (left, corresponding to Table 3S in the Supporting Information and Figure 9) and their arithmetic average (right).

experimental minima at 1314 and 1279 cm^{-1} (calcd at 1287 and 1258 cm^{-1}). Also the experimental VCD bands at 1262, 1215, 1175, 1109, and 1088 cm^{-1} correspond most probably to the calculated peaks of the same signs at 1241, 1212, 1156, 1090, and 1063 cm^{-1}, respectively. Presumably, for a complete averaging, the VCD signal from the benzoyl C═O groups (calculated around 1728 cm^{-1}) would disappear completely, while the lactone ring C═O group stretching provides a net positive VCD signal, observed in the experimental spectrum in this region. The averaged VCD spectrum is less intense than the individual components (see the vertical scale in Figure 10), which reflects well-known difficulties with the measurement of flexible compounds.

Conclusions

The chiral Corey lactone chromophore could be recognized in the VCD and absorption spectra of the derivatives. However, it forms their minor component. The lactone side groups influence the VCD signal significantly, depending on the conformational flexibility and the ability to form inter- and intramolecular hydrogen bonds, which can be used backward in order to obtain structural information from the spectra. The diol **A** interacts strongly with the solvent, but a preferred conformation exists. The alcohols **B** and **C** adopt conformations stabilized by an internal hydrogen bond, while the bisbenzoate **D** exhibits a free movement of the functional groups. This different flexibility is consistent with the interpretation of the experimental spectra based on ab initio calculation, providing a good agreement of signs, relative intensities, and transitional frequencies.

Experimental Section

We studied four compounds: (1*R*,5*S*,6*S*,7*S*)-(+)-7-hydroxy-6-hydroxymethyl-2-oxabicyclo[3.3.0]octan-3-one (or as known by its trivial name "(+)-Corey lactone diol", **A**); (1*R*,5*S*,6*S*,7*S*)-(+)-7-(phenyl-4-oxycarbonyl)-6-hydroxymethyl-2-oxabicyclo-[3.3.0]octan-3-one ("(+)-Corey lactone benzoate alcohol", **B**); (1*R*,5*S*,6*S*,7*S*)-(+)-7-(1,1′-biphenyl-4-oxycarbonyl)-6-hydroxymethyl-2-oxabicyclo[3.3.0]octan-3-one ("(+)-Corey lactone *p*-phenylbenzoate alcohol", **C**); (1*R*,5*S*,6*S*,7*S*)-(−)-7-benzoyloxy-6-benzoyloxymethyl-2-oxabicyclo[3.3.0]octan-3-one ("(−)-Corey lactone bisbenzoate", **D**). See Figure 1 for the structures. For **A**, **B**, and **D**, optical antipodes were also available, which could be used for determining and eliminating artifacts from their VCD spectra.[20] Thus, their experimental spectra were obtained as half of the difference spectrum of the (+) and (−) enantiomers. For **C**, the VCD spectrum of the racemate was subtracted from the VCD of the (+) form. All chemicals were of 98% purity or higher. The VCD and infrared absorption spectra were recorded simultaneously with a spectral resolution of 4 cm^{-1} on a IFS 66/S FTIR spectrometer. A low-pass filter (<1800 cm^{-1}), BaF_2 polarizer, ZnSe modulator operating at 50 kHz, and MCT detector were used. The experimental setup and instrument performance have been described in detail elsewhere.[21] Sample **A** was dissolved in D_2O (99.9%) at a concentration of 0.6 mol L^{-1}, and samples **B**−**D** in $CDCl_3$ (>99%) were dissolved at concentrations in the interval of 0.15−0.37 mol L^{-1}. Demountable KBr and CaF_2 cells were used with 50 and 25 μm Teflon spacers for $CDCl_3$ and D_2O solutions, respectively. The VCD spectra were obtained as an average of three blocks of 3380 scans.

Calculations

Starting geometries for the ensemble of conformers for all of the four derivatives were generated using the Hyperchem[22] and Spartan[23] software packages via a systematic change of torsion angles of the freely rotating bonds. Low-energy conformers were preselected on the basis of the MM and PM3[24] methods and then optimized at the BPW91/6-31G** DFT level[25] using the Gaussian 98[12] software. For equilibrium geometries, harmonic frequencies and rotational and dipolar strengths were calculated, and IR and VCD spectral intensities were simulated using Lorentzian bands of a bandwidth of 5 cm^{-1}.

Acknowledgment. This work was supported by the Ministry of Education, Youth and Sports of the Czech Republic (CEZ: MSM 223400008), the Grant Agency of the Academy of Sciences (A4055104), and the Grant Agency of the Czech Republic (203/01/0031). We thank Prof. T. A. Keiderling for valuable discussion on the topic and V. Borek and I. Veselý for technical assistence.

Supporting Information Available: Conformer energies, IR and VCD spectral intensities, and Cartesian coordinates. This material is available free of charge via the Internet at http://pubs.acs.org.

JO035099H

(20) Keiderling, T. In *Practical Fourier Transform Infrared Spectroscopy*; Ferraro, J. R., Krishnan, K., Eds.; Academic: San Diego, CA, 1990; pp 203−284.
(21) Urbanová, M.; Setnička, V.; Volka, K. *Chirality* **2000**, *12*, 199.
(22) *HyperChem*7; Hypercube, Inc.: Gainesville, FL, 2002.
(23) *SpartanPC Pro*; Wavefunction, Inc.: Irvine, CA, 2000.
(24) Stewart, J. J. P. *J. Comput. Chem.* **1989**, *10*, 209.
(25) Perdew, J. P.; Chevary, J. A.; Vosko, S. H.; Jackson, K. A.; Pederson, M. R.; Fiolhais, C. *Phys. Rev. B: Condens. Matter Mater. Phys.* **1992**, *46*, 6671.